Design and analysis of collision reduction algorithms for LED-based indoor positioning with simulation and experimental validation

Popoola, Olaoluwa R.; Sinanovic, Sinan

Published in:
IEEE Access

DOI:
10.1109/ACCESS.2018.2801626

Publication date:
2018

Document Version
Peer reviewed version

This article has been accepted for publication in a future issue of this journal, but has not been fully edited. Content may change prior to final publication. Citation information: DOI 10.1109/ACCESS.2018.2801626, IEEE Access

Design and Analysis of Collision Reduction Algorithms for LED-based Indoor Positioning with Simulation and Experimental Validation

Olaoluwa R. Popoola* and Sinan Sinanović*
*School of Engineering and Built Environment, Glasgow Caledonian University, Glasgow, G4 0BA, UK
Email: {olaoluwa.popoola, sinan.sinanovic}@gcu.ac.uk

***Abstract*—In this work, we develop a low complexity indoor positioning system (IPS) and design a lightweight, low-cost and wearable receiver for it. The accuracy of proximity-based LED IPS has been improved using overlap between LED beams but LED packets in the overlap region are subject to collisions. In this work, we design collision handling algorithms for the IPS that considers building and lighting infrastructures. Mathematical analyses of the proposed algorithms are done and models for the probability of collisions are developed. The models, which are verified using simulations, are used to calculate the time required for position update called positioning time. Analysis of the positioning time is done for single and multiple receivers systems and validated with experimental measurements. Results show positioning error as low as 56 cm with a positioning time of about 300 ms for slotted unsynchronized systems and 500 ms for unslotted unsynchronized systems which makes the developed system pragmatic and appropriate for human positioning.**

***Keywords*–** Collision reduction, Indoor, Light emitting diodes, Localization, Microcontroller, Overlap, Positioning, Unsynchronized, Wearable.

I. Introduction

Global navigation satellite system (GNSS) has witnessed tremendous success in positioning as it is currently easily integrable with various mobile phones, cars, and other similar devices. In these devices, the GNSS works by receiving positional signals from four satellites. In an outdoor environment, these signals are readily available and provide satisfactory accuracy [1]–[3]. However, in indoor or enclosed environments, the positional signals suffer from attenuation by walls and scattering from indoor objects [4]. Consequently, the resulting positional signal received by the global positioning signal (GPS) chip is not good enough to provide accurate information indoors. The deficiency of positional signals in indoor environments led to ongoing research work both in the academia and industry to develop indoor positioning systems (IPS). Literature survey shows that most techniques used in indoor positioning are based on inertial sensors, signal parameter variation or signal mapping [5]–[8].

Indoor positioning based on inertial sensors use accelerometers and gyroscopes to measure the acceleration and angular velocity of the sensor. The changes in both quantities are used to derive the deviation in position as an object moves from one position to another. This approach works on the assumption that the start point is known and the movement profile measured by the inertial sensor is used to predict the endpoint or the position of an object. In order to know start points, inertial sensors based positioning is used with signal mapping or signal parameter variation [7].

Indoor positioning systems based on signal parameter variation sets up a communication link between one or more transmitters and one or more receivers. The indoor position is subsequently determined by the variation of one or more of the communication signal parameters. Communication signal parameter refers to any parameter of a communication signal which changes in value as the signal travels. Various communication signal parameters that have been investigated for indoor positioning purposes include the received signal strength (RSS) [8], the angle of arrival (AoA) [9], time of arrival (ToA), time difference of arrival (TDoA) [10], and phase difference of arrival (PDoA). The communication link can be based on radio frequency (RF), ultrasound [11], magnetic sensors [12] or light [13], [14]. RF-based communication links have been investigated for indoor positioning using Bluetooth protocols [15], RFID, Zigbee [16], WiFi and ultra wide band (UWB) [7]. Ultrasound technology sets up a communication link between a high-frequency sound transmitter and receiver while magnetic sensors use magnetic/inductive effects [11]. Light-based communication links or optical wireless communications (OWC) is made possible by the use of optical signals to set up a wireless link between an optical transmitter and receiver [17].

In signal mapping based IPS, signals from a reference point are broadcast and the received signal profile at different points are mapped [5], [6]. This map serves as a fingerprint and this method is popularly known as positioning by fingerprinting. In order to determine the location of an object or person, the signal profile is checked against the fingerprint and the location where there is the highest similarity is predicted as the estimate. A less complicated signal mapping method is proximity positioning. In proximity positioning, the content of the signal is used to infer positions directly [18].

Investigations on the applicability of light in positioning by signal variation in terms of RSS, ToA, AoA, TDoA and PDoA led to the development of various IPS which show appreciable levels of accuracy but the systems developed are either too expensive or inapplicable to practical scenarios [17]. Positioning by fingerprinting requires a pre-phase for capturing map features and fingerprinting based positioning systems have to be redesigned when the environmental changes [19].

This article has been accepted for publication in a future issue of this journal, but has not been fully edited. Content may change prior to final publication. Citation information: DOI 10.1109/ACCESS.2018.2801626, IEEE Access

Unlike the aforementioned systems, proximity-based IPS are hardware friendly, inexpensive to implement and less dependent on environment changes. However, the accuracy of proximity-based IPS is poor since the error in positioning is proportional to the size of a room or the coverage area of the LED used called the LED footprint [18].

To address the shortcoming of proximity-based IPS, a novel indoor positioning method called the multiple LED estimation model (MLEM) is introduced in [17]. MLEM uses overlaps of LED footprints to increase the accuracy of positioning irrespective of the room size or the LED footprint. Fig. 1a shows an indoor location where overlap is used to increase the number of regions detectable by a mobile receiver (Mrx) from two to three. By increasing the number of LEDs, the accuracy of proximity-based positioning is shown to increase significantly in [17], [20]. Based on the simple proximity-based architecture, prototypes of MLEM IPS are portable, wearable and built using off-the-shelf components [17]. However, in regions of overlapping LED beams, LED data carrying packets are subject to collisions. When collisions occur, data packets are destroyed. Application of existing RF-based collision handling schemes such as code division multiple access (CDMA) to this OWC-based system requires specialized hardware and the resulting IPS are expensive, bulky and unwearable which defeats the purpose of proximity-based IPS. The Aloha protocol which is a simple RF based collision handling protocol is also not applicable because the ALOHA protocol works by the use of a received 'ACK' acknowledgement packet by a transmitting system [21]. This differs from our system in two ways; first, the receiver photodetector (PD) system only receives optical signals and is not designed to transmit any optical signal. Secondly, the LED transmits optical signals in a simplex communication such that they only transmit and do not receive. Therefore there is a need to develop a positioning algorithm which handles collision in overlapping region of LED beams without trading off the advantages of MLEM as an improved proximity-based IPS.

This paper examines collision handling in MLEM-IPS by considering four lighting system designs which are synchronized system, semi-synchronized system, slotted unsynchronized system and unslotted unsynchronized system. This is achieved by analysis confirmed with simulations and partly with experiments. Whereas the synchronized system is akin to time division multiplexing (TDM), this paper introduces novel collision handling schemes in semi-synchronized, slotted unsynchronized and unslotted unsynchronized OWC-based systems in regions of overlap. This is carried out by deriving the probability of collision for various numbers of overlaps in all four types of lighting system designs. The positioning time, defined as the time taken for the receiver to locate itself, is then computed using the models of probability of collision developed. The computed time is used as a performance metric to compare collision handling performance of the four designs. To further improve the accuracy of positioning, the collision algorithm is extended to a MLEM multiple receiver IPS.

The rest of the paper is organized as follows: the system model is described in Section II, MLEM single receiver and the lighting system design for the implementation of the MLEM system is considered in Section III. Multiple receiver MLEM positioning is considered in Section IV where its effect on positioning is presented in Section IV-A and its positioning time calculated in Section V. System performance, results and experimental validations are presented in Section VI and finally, in Section VII conclusions are presented.

II. System Model Description

The system sets up an optical link between a LED transmitter and a Mrx in an overlap region as illustrated in Fig. 1a. The Mrx is a PD with a small microcontroller attached to a person or an object whose position is to be determined. Fig. 1b shows the system environment which is an arbitrary indoor location of dimension 5m $\times$ 5m $\times$ 3m for four overlapping circular light beams.

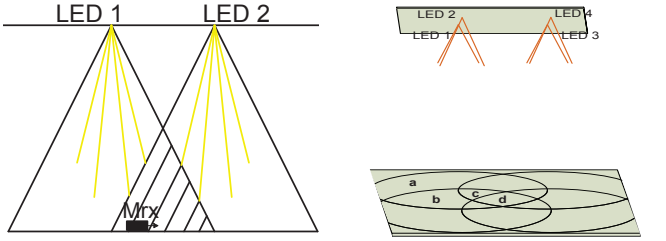

(a) Illustration of overlap region where LED data packets are subject to collision.

(b) Example of different overlap regions

Fig. 1: Various overlap conditions obtainable from the system under consideration

The Mrx determines its position based on the LED data received with line of sight (LOS) serving as the primary communication link for this investigation. The optical power received by the Mrx from a single LED without overlap, P_{rx}, is given in [22], [23] as:

$$P_{rx} = \begin{cases} P_{tx}\frac{\mathfrak{m}+1}{2\pi d^2} A \cos^{\mathfrak{m}}(\phi) T_s(\varphi) g(\varphi) \cos(\varphi), & 0 \leq \varphi \leq \varphi_c \\ 0, & \varphi > \varphi_c \end{cases} \tag{1}$$

where A is the physical area of the PD, d is the LOS distance between the transmitter and the receiver, ϕ is the angle of irradiance with respect to the transmitter perpendicular axis, φ is the angle of incidence and P_{tx} is the optical power transmitted from a LED with parameters given in Table I. $T_s(\varphi)$ is the gain of an optical filter, φ_c is the field of vision of the receiver, $g(\varphi)$ is the gain of the optical concentrator given as a proportion of the refractive index $\mathfrak{n}$ as:

$$g(\varphi) = \begin{cases} \frac{\mathfrak{n}^2}{\sin^2 \varphi_c}, & 0 \leq \varphi \leq \varphi_c \\ 0, & \varphi > \varphi_c \end{cases} \tag{2}$$

$\mathfrak{m}$ is the order of the Lambertian source and is:

$$\mathfrak{m} = \frac{\ln(1/2)}{\ln(\cos(\Phi_{1/2}))} \tag{3}$$

where $\Phi_{1/2}$ is the half angle.

Based on the equations, the simulation parameters shown in Table I and assuming unity gain for the optical filter, the

This article has been accepted for publication in a future issue of this journal, but has not been fully edited. Content may change prior to final publication. Citation information: DOI 10.1109/ACCESS.2018.2801626, IEEE Access

received optical power profile reveals four possible overlap regions as illustrated in Fig. 1b. Therefore, the receiver in such scenario is subject to different possible overlap regions depending on the number of sources from which the optical power is detectable. In region **a**, based on the footprint of the LEDs, the Mrx receives data from only one source. The footprint of the LEDs defines the region on a horizontal plane where the optical power from a particular LED is detectable. If a receiver is in this region, **a**, the receiver assumes the coordinate of the LED which covers the region. In region **b**, the receiver detects light from two sources and the receiver assumes the midpoint of the coordinates of both LEDs which covers that region. Light is detected from three sources in region **c** and four in region **d** and midpoints of the three and four LEDs are used to assume the position of the receiver. These regions are used in the various MLEM implementation designs described in Section III.

TABLE I: Parameters of components and devices used for experiment and simulations in this work

Parameters	
Light emitting diode (LED)	OSRAM IR LED (LD 271)
angle of half intensity $\varphi_{1/2}$	$\pm 25^{o}$
peak wavelength λ_p	950 nm
total radiant flux ϕ_a	18 mW
rise and fall time t_r,t_{fa}	1 μs
Photodetector (PD)	VISHAY (TSOP 38238)
Directivity (θ)	45°
Peak wavelength λ_p	950 nm
Minimum irradiance $E_{(emin)}$	0.12 mW/m^2
Detector physical area	1 cm^2
Refractive index $\mathfrak{n}$	1.5
Field of Vision φ_c	60°
Oscilloscope	Agilent (DSO-X 3034A)

III. Single receiver MLEM implementation designs

In this section, the different practical designs for the implementation of an MLEM IPS are investigated. This section focusses on investigation with single receivers in order to establish the theoretical relationships for the packet duration multiplexing (PDM) collision avoidance algorithm. In the next section, these relationships are extended to multiple receiver MLEM systems which are used to further increase the accuracy of positioning. The structure for deployment of LED lights could assume three forms. First, LED lights could be set up with a timed controller such that a time division multiplexing (TDM) scheme is set up between the transmitters. This is considered as a synchronized system. A semi-synchronized system is considered second and finally, random access unsynchronized systems are considered.

A. Synchronized system - best case scenario

This system implements TDM between a number of LEDs for positioning. It sets up a central clock that performs time-sharing for the LEDs. Therefore, each of the individual LED transmits its packet in a particular time slot. The central clock is designed to allow individual LED to send a data packet before handing over to another LED. A position carrying data packet from each LED, when received by the Mrx, denotes that LED as one of the transmitting sources in that region. Consider a scenario for a synchronized system using four LEDs, LED 1, LED 2, LED 3 and LED 4 as shown in Fig. 2. The receiver is designed to predict location when it receives data from a particular source twice. This is done to make the Mrx scalable and adaptable to increasing number of overlaps because the central clock allows every other LED in the enclosure to transmit all their packets before allowing an LED to transmit its packet the second time. Therefore, the positioning time is the time taken for the receiver to receive the data packet from a LED twice. Since the central clock allows each LED to transmit only one packet per allocated time, the receiver in a non-overlapping region requires the first packet from the LED in that region, and the second packet from the same LED. For instance, in region **a**, since data from other LEDs are off in this region, the receiver would receive $LED1data, blank, blank, blank, LED1data$ where $blank$ represents no data received. In region **c**, the receiver receives a sequence like $LED1data, LED2data, LED3data, blank, LED1data$ since optical signals from LED 4 do not cover this region. This received data is subsequently used to predict position by the receiver.

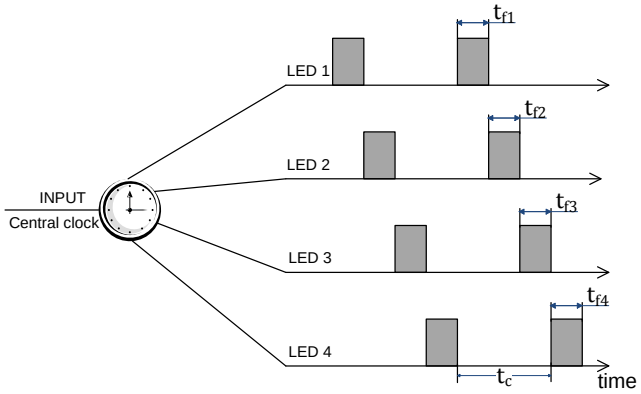

Fig. 2: Central controller for the synchronized system

The probability of collision in all regions (**a**,**b**,**c**,**d**) is 0 because the packets are separated in time. The positioning time is the sum of time for transmission of all packets in the system plus time of re-transmission of the first packet. If t_f is the time it takes a transmitter to send a data packet such that t_{fi} is the time it takes the LED i transmitter to send its data packet, for the 4-LED system under consideration, if LED 1 sends its data first, the positioning time $t_{p4} = 2t_{f1} + t_{f2} + t_{f3} + t_{f4}$. Consequently, the positioning time for this synchronized system for N LEDs, t_{pN} is given by:

$$t_{pN} = t_{f1} + \sum_{i=1}^{N} t_{fi} \tag{4}$$

This article has been accepted for publication in a future issue of this journal, but has not been fully edited. Content may change prior to final publication. Citation information: DOI 10.1109/ACCESS.2018.2801626, IEEE Access

Although this system gives the lowest positioning time, it may be difficult to implement practically as it requires a re-design of existing building infrastructure and/or the rewiring of lighting facilities to include a central controller. The drawbacks of this system lead to a modified version called the semi-synchronized system described in Section III-B.

B. Semi-synchronized system

The semi-synchronized system is a more practical form of the synchronized system. In this system, the central controller used in the synchronized system is made abstract by transferring operations to software. This system operates with the assumption that all the lights in an enclosure are turned on or off by a single switch as is often the case in modern lighting designs. Collision prevention between packets is achieved by including a delay between LED transmitters as illustrated in Fig. 3.

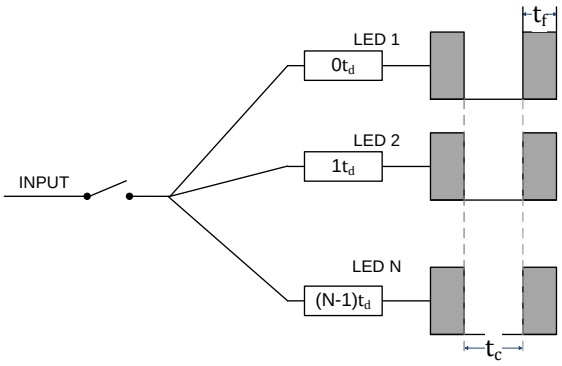

Fig. 3: Semi-synchronized system using gang switch

In Fig. 3, t_d represents a chosen delay time and t_c represents the cycle time which is also the time interval between transmissions of two successive packets from a single LED. The delays are used to implement an offset between data packets from one LED and that from another LED. The offset between the packet transmission times from a single LED also acts to prevent the collision by allocating enough time for other LEDs to transmit their packets. For simplicity in analysis and implementation, all LEDs are assumed to be of the same packet size such that t_f is the same for all LEDs. Based on this assumption, for a system of N LEDs, the minimum cycle time required for the implementation of a semi-synchronized system is:

$$t_{c\_min} = Nt_f. \tag{5}$$

The minimum value of delay time t_{d_min} to avoid repeated collisions is t_f. For this system, the probability of collision of data packets is 0 and the positioning time is the sum of the implemented delay t_d and the cycle time t_c. Therefore, the minimum positioning time in an enclosed area of N LEDs is given by:

$$t_{pN\_min} = (N+1)t_f. \tag{6}$$

The semi-synchronized system offers a easier-to-implement version of the MLEM system with no possibility of collision. However, the assumption that every LED luminaire in an enclosed space is controlled by a single switch may not hold true for all lighting designs. In addition, the semi-synchronized system requires that a specified delay is programmed into each LED luminaire. This could be achieved by adding delay label tags to LED transmitters. This approach, however, is not applicable to all practical cases. Consequently, cases for individual unsynchronized light switches are investigated in the next section.

C. Unsynchronized systems

In this section, the MLEM design is implemented without synchronization between transmitters. We consider non-synchronization in two possible forms. First is a slotted unsynchronized system which addresses the need for delay label tags to LED transmitters in the semi-synchronized system and next we consider an unslotted and unsynchronized design. The slotted unsynchronized system considers a system with a central switch but without any form of correlation between LED delays among transmitter LEDs while the unslotted unsynchronized system considers a system with non-central switch and no correlation between delays. To reduce collision in these systems, the LED data carrying packets are sent once in a cycle time. The cycle time is the sum of time taken for a LED to transmit its packet and the time the LED is required to stay off.

1) Slotted unsynchronized system: In this system, unsynchronized LEDs transmit data in slots chosen randomly. To put data in slots, all LEDs are assumed to be in the same room, identical and operate on a delay function which is dependent on a random value as illustrated in Fig. 4. The random value is generated by the integer function $R(k)$ which randomly selects an integer between the set of numbers $[1, 2, ..., k]$ and k is dependent on the transmission duty cycle D given by:

$$D = \frac{t_f}{t_f + t_{off}} = \frac{t_f}{t_c} = \frac{1}{k} \tag{7}$$

where t_{off} is the minimum time between two successive packet transmissions from the same LED. The values of t_f and t_{off} are selected so that the fraction $\frac{t_f + t_{off}}{t_f}$ produces an integer value k which represents the inverse of the duty cycle. The integer random function R allows LED packets

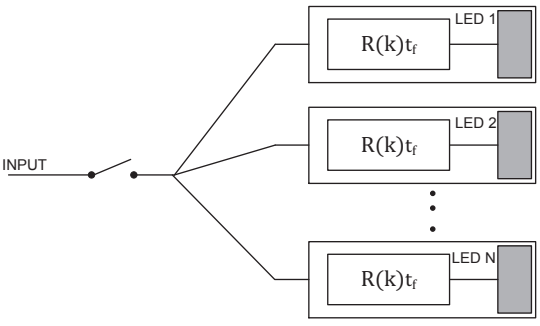

Fig. 4: Slotted unsynchronized system with random delays

to be transmitted at randomly chosen slots as illustrated in

This article has been accepted for publication in a future issue of this journal, but has not been fully edited. Content may change prior to final publication. Citation information: DOI 10.1109/ACCESS.2018.2801626, IEEE Access

Fig. 5. Consequently, there is a probability of collision for the slotted unsynchronized system and the probability of collision is dependent on how many LEDs are in a particular region. Therefore, unlike the systems in Section III-A and Section III-B, this system has a different probability of collision of packets for the Mrx in region **a**, region **b**, region **c** or in region **d**. In region **a**, there is only one LED participating in data transmission, therefore, the probability of collision is 0. In region **b**, there are two LEDs participating in data transmission. If one of the LEDs, say LED 1, transmits at a duty cycle D such that its data packet is in one of k possible slots and LED 1 uses only one of the slots in a transmission cycle, then for no collision, the other LED say LED 2, has $(k-1)$ possible slots for transmission as illustrated in Fig. 5. If P_{ncsN} represents the probability of no collision of N slotted

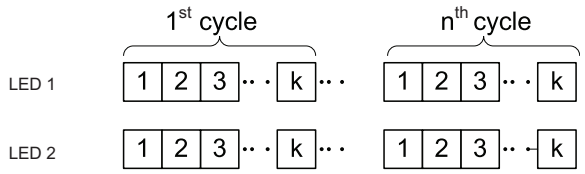

Fig. 5: Illustration of slots and cycles for packet transmission

LEDs and P_{csN} represents the probability of collision of N LEDs in a slotted unsysnchronized system, the probability of collision, P_{csN} is given as $1 - P_{ncsN}$. In the region **b**, the probability of no collision for two slotted LEDs is expressed as:

$$P_{ncs2} = \frac{k-1}{k}. \tag{8}$$

Therefore, the probability of collision for packets in this region, or in any overlap region with only two LEDs is given as:

$$P_{cs2} = \frac{1}{k}. \tag{9}$$

For region **c** with three LEDs, given k slots where the first LED transmits data in one of the k slots, to avoid collision, the second LED has to transmit its data in one of $(k-1)$ slots and the third LED has $(k-2)$ slots left for data transmission. The probability of no collision in this region is given by $P_{ncs3} = \frac{(k-1)(k-2)}{k^2}$. The probability of collision is therefore given as:

$$P_{cs3} = 1 - \frac{(k-1)(k-2)}{k^2}. \tag{10}$$

In an overlap region of four LEDs (region **d**), by similar argument, the probability of collision is given as:

$$P_{cs4} = 1 - \frac{(k-1)(k-2)(k-3)}{k^3}. \tag{11}$$

In general, the probability of collision in an overlap region with N LEDs transmitting data over k possible slots is given as:

$$P_{csN} = 1 - \frac{(k-1)!}{k^{N-1}(k-N)!} = 1 - \prod_{i=1}^{N-1} \frac{k-i}{k} \tag{12}$$

and the probability of no collision is:

$$P_{ncsN} = \frac{(k-1)!}{k^{N-1}(k-N)!} = \prod_{i=1}^{N-1} \frac{k-i}{k}. \tag{13}$$

In terms of the cycle time t_c, by substituting from (7), the probability of no collision of a slotted unsynchronized system can be written as:

$$P_{ncsN} = \prod_{i=1}^{N-1} \frac{t_c - t_f}{t_c} \tag{14}$$

and the probability of collision is:

$$P_{csN} = 1 - \prod_{i=1}^{N-1} \frac{t_c - t_f}{t_c}. \tag{15}$$

Due to the non-zero probability of collision for this system, the positioning time depends on whether a collision occurs or not. Therefore, the average positioning time (APT) is computed as a metric for the positioning time. Consequently, the APT $\bar{t}_{ps}$ given by:

$$\bar{t}_{ps} = \bar{t}_{pncs} P_{ncsN} + \bar{t}_{pcs} P_{csN} \tag{16}$$

is used for simulations where $\bar{t}_{pncs}$ is the APT without collision and $\bar{t}_{pcs}$ is the APT with collision. The positioning time when no collision occurs is the time taken to receive all packets in the enclosed area. Since all packets are placed in slots for every transmission cycle, and detection is done by Mrx receiving one of the data packets twice, the second packet from any LED could be in any slot ranging from the first slot to the k-th slot in the second cycle. Consequently $\bar{t}_{pncs}$ ranges between $kt_f + t_f$ and $2kt_f$. For this work, we assume the APT when no collision occurs as the mean of the two extremes. Therefore $\bar{t}_{pncs}$ can be written as:

$$\bar{t}_{pncs} = \frac{(3k+1)t_f}{2} = \frac{3t_c + t_f}{2}. \tag{17}$$

When collision occurs, the positioning time is computed based on the number of transmission cycles that guarantees that packets from all LEDs in the region are received. If for a particular duty cycle D, the probability of collision occurring in a transmission cycle is given by P_{csN}, the probability that collision occurs in all n_c-cycles is therefore $P_{csN}^{n_c}$. The probability that collision does not occur in at least one of the cycles is given by $1 - P_{csN}^{n_c}$. The required number of cycles that guarantees s success rate for a no-collision cycle is therefore given by:

$$n_c = \frac{\log(1-s)}{\log(P_{csN})}, \qquad 0 < s < 1. \tag{18}$$

To guarantee a high success rate, s is taken to be 0.9999 which gives the number of cycles that ensures a 99.99% chance that a no-collision cycle occurs. Consequently, the positioning time when a collision occurs is given as $\bar{t}_{pcs} = n_c \bar{t}_{pncs}$. By substituting the values of $\bar{t}_{pncs}$, P_{ncsN}, $\bar{t}_{pcs}$ and, P_{csN}, the APT can be written as:

$$\bar{t}_{ps} = \left(\frac{3t_c + t_f}{2}\right)\left(\prod_{i=1}^{N-1} \frac{t_c - t_f}{t_c}(1 - n_c) + n_c\right). \tag{19}$$

The slotted unsynchronized implementation of the MLEM system represents a more realistic technique because it eliminates the specific delays programmed to LEDs. Therefore any LED can be programmed independently. Unlike the previous systems, this system is subject to collisions. However, by

This article has been accepted for publication in a future issue of this journal, but has not been fully edited. Content may change prior to final publication. Citation information: DOI 10.1109/ACCESS.2018.2801626, IEEE Access

appropriately selecting the cycle time t_c, the probability of collision can be appreciably reduced as simulations in Section VI show.

2) Unslotted unsynchronized system: In this section, the investigation of the MLEM design for lighting solutions where each luminaire is controlled by a separate switch is considered. Separate controls for light sources make use of slotting difficult so systems with no central control are considered here as unslotted unsynchronized systems. By modifying (7), the transmission duty cycle of this system can be written as:

$$D = \frac{1}{\hat{k}} \tag{20}$$

where $\hat{k}$ is the inverse of duty cycle and not necessarily an integer. In this system, the lack of any form of central control means data is not transmitted in slots but can be sent at any random time. Fig. 6 shows the unslotted unsynchronized system where $R(t_c)$ is used to place packets from different LED sources in different time intervals to avoid collisions. Considering Fig. 1b, in region **a**, since only one LED transmits

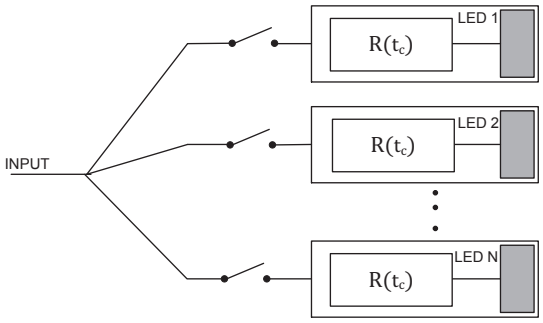

Fig. 6: Structure for the unslotted unsynchronized system showing no form of coordination among LEDs

in that region like in the case for slotted synchronized systems, the probability of collision is zero. In the region **b**, with two LEDs transmitting packets of the same size, over a low duty cycle D, according to [17], if one of the LEDs (say LED 1) transmits its data packet of duration t_f at a particular point in the period of transmission $t_c = t_f + t_{off}$ the other LED in this region (say LED 2) has a $t_c - 2t_f$ interval to transmit its data. If P_{ncuN} represents the probability of no collision of N unslotted LEDs and P_{cuN} represents the probability of collision of N LEDs in an unslotted unsysnchronized system, the probability of no collision in this region is given by $P_{ncu2} = \frac{t_c - 2t_f}{t_c}$. By appropriate substitution from (20), P_{ncu2} can be written as:

$$P_{ncu2} = \frac{\hat{k} - 2}{\hat{k}} \tag{21}$$

and the probability of collision in this region $P_{cu2} = 1 - P_{ncu2} = 2/\hat{k}$.

In a region of overlap between three LEDs, to avoid collision, packets from all three LEDs and packets from any two LEDs must not be transmitted at the same time. For packets from all three LED, no collision occurs if data packet from LED 1 is at a point in the cycle that occupies an interval t_f, data packet from LED 2 can only be within any of $t_c - 2t_f$ points in the cycle and packets from LED 3 can only be within $t_c - 3t_f$ points in the cycle. The probability of no collision between packets from all three LEDs is therefore $P_{all_3} = \frac{t_c - 2t_f}{t_c}\frac{t_c - 3t_f}{t_c}$. The probability of no collision between data packets from any two LEDs (say LED 1 and LED 2) is the probability of no collision when data packets from LED 1 and LED 2 are not in the same interval where the three LEDs collide. That is LED 2 data packet is in an interval $t_c - 2t_f$ and LED 1 data packet is in an interval $t_c - t_f$ out of LED 2's packet $t_c - 2t_f$ interval. The probability of no collision among any two LEDs is given as $P_{any_2} = \frac{t_c - t_f}{t_c - 2t_f}\frac{t_c - 2t_f}{t_c}$. The probability of no collision in this region is therefore given as $P_{ncu3} = P_{all_3}P_{any_2} = \frac{t_c - t_f}{t_c}\frac{t_c - 2t_f}{t_c}\frac{t_c - 3t_f}{t_c}$ simplifying according to (7), the probability of no collision in region of three LEDs can be written in terms of $\hat{k}$ as:

$$P_{ncu3} = \frac{(\hat{k}-1)(\hat{k}-2)(\hat{k}-3)}{\hat{k}^3}. \tag{22}$$

By a similar analysis, the probability of no collision in region **d**, is given by:

$$P_{ncu4} = \frac{(\hat{k}-1)(\hat{k}-2)^2(\hat{k}-3)(\hat{k}-4)}{\hat{k}^5} \tag{23}$$

Generally, the probability of no collision for the unslotted unsynchronized system in N overlap region can be written as:

$$P_{ncuN} = \frac{(\hat{k}-1)!(\hat{k}-2)!}{\hat{k}^{(2N-3)}(\hat{k}-N-1)!(\hat{k}-N+1)!} \tag{24}$$

and the probability of collision between packets is given by $P_{cuN} = 1 - P_{ncuN}$ can be written as:

$$P_{cuN} = 1 - \frac{(\hat{k}-1)!(\hat{k}-2)!}{\hat{k}^{(2N-3)}(\hat{k}-N-1)!(\hat{k}-N+1)!}. \tag{25}$$

In terms of cycle time, the probability of no collision for the unslotted unsynchronized system in N overlap region is:

$$P_{ncuN} = \frac{t_f^{2N-3}(t_c - t_f)!(t_c - 2t_f)!}{t_c^{2N-3}(t_c - Nt_f - t_f)!(t_c - Nt_f + t_f)!} \tag{26}$$

and the probability of collision is given by:

$$P_{cuN} = 1 - \frac{t_f^{2N-3}(t_c - t_f)!(t_c - 2t_f)!}{t_c^{2N-3}(t_c - Nt_f - t_f)!(t_c - Nt_f + t_f)!}. \tag{27}$$

The APT for this system given as:

$$\bar{t}_{pu} = \bar{t}_{pncu}P_{ncuN} + \bar{t}_{pcu}P_{cuN} \tag{28}$$

depends on the APT when no collision occurs, $\bar{t}_{pncu}$, and that when a collision occurs $\bar{t}_{pcu}$. When no collision occurs, the positioning time is similar to that of the slotted unsynchronized system since the detection method is similar. The positioning time when no collision occurs can be written by using (17) as $\bar{t}_{pncu} = \frac{(3t_c + t_f)}{2}$. When collision occurs, by a similar argument as in Section III-C1, the positioning time can be written as $\bar{t}_{pcu} = \log_{P_c}(1-s)\bar{t}_{pncu} = n_c\bar{t}_{pncu}$. Substituting the values of $\bar{t}_{pcu}$, $\bar{t}_{pncu}$, P_{ncuN} and P_{cuN} into (28) gives the APT for the unslotted unsynchronized system as:

$$\bar{t}_{pu} = \frac{3t_c + t_f}{2}\left[\frac{(1-n_c)(t_c - t_f)!(t_c - 2t_f)!t_f^{2N-3}}{(t_c - Nt_f - t_f)!(t_c - Nt_f + t_f)!t_c^{2N-3}} + n_c\right]. \tag{29}$$

This article has been accepted for publication in a future issue of this journal, but has not been fully edited. Content may change prior to final publication. Citation information: DOI 10.1109/ACCESS.2018.2801626, IEEE Access

D. APT for a mobile single receiver

In Section III, stationary receivers in specific overlap regions are considered. However, a person wearing the receiver in the room, moves across various overlap region. The APT of the receiver in this scenario is computed in this section as the APT of a mobile single receiver. To simplify analysis, we use a transmitter orientation where the LED transmitters are assumed to be identical such that the radius of the optical footprint from each LED is the same. In addition, the LED transmitters uniformly distributed and arranged in such a way that the center of each LED is on the circumference of another LED footprint. Using the room dimensions 5m × 5m × 3m from Section II, this setup for two, three and four LED transmitters is illustrated in Fig. 7.

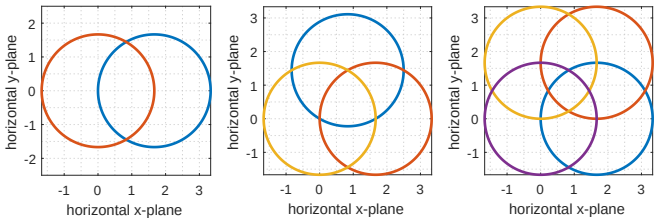

Fig. 7: Illustration of LED arrangements for investigating the APT of mobile single and multiple receivers

Considering a scenario for a two transmitter system, the APT is dependent on the positioning time at a no-overlap region and the positioning time at a two LED overlap region. This positioning time is based on the geometrical probability that a receiver is in a certain overlap region. By using the transmitter arrangements in Fig. 7, if $\bar{t}_{mn}$ represents the APT in an overlap region with m receivers and n transmitters such that $m = 1$ for a single receiver and $1 \leq n \leq N$, when $N = 2$, the APT can be written as:

$$\bar{t}_{12} = \bar{t}_{p11}\frac{A_{12}}{A_{2t}} + \bar{t}_{p12}\frac{A_{22}}{A_{2t}} \tag{30}$$

where $\bar{t}_{12}$ is the APT of a system with one receiver and two transmitters, $\bar{t}_{p1n}$ is the APT of a stationary receiver in n LED transmitter overlap region so that $\bar{t}_{p1n} = \bar{t}_{pN}$ for synchronized systems, $\bar{t}_{p1n} = \bar{t}_{pN\_min}$ for semi-synchronized systems, $\bar{t}_{p1n} = \bar{t}_{ps}$ for slotted unsynchronized systems, $\bar{t}_{p1n} = \bar{t}_{pu}$ for unslotted unsynchronized systems, A_{nN} is the area of n overlapping LEDs in a system of N transmitters and A_{Nt} is the total area covered by the system with N transmitters which can be expressed as:

$$A_{Nt} = \sum_{n=1}^{N} A_{nN} \tag{31}$$

The values of these areas can be computed by considering the geometry of the overlap system. Considering the overlap system in Fig. 7, the ratio of areas of overlap regions to the total area of a system is represented in Table II (see derivation in Appendix A).

TABLE II: Ratio of areas of various overlap regions to the total area covered by N LED transmitters

	$\frac{A_{1N}}{A_{Nt}}$	$\frac{A_{2N}}{A_{Nt}}$	$\frac{A_{3N}}{A_{Nt}}$	$\frac{A_{4N}}{A_{Nt}}$
$N = 1$	1	-	-	-
$N = 2$	0.76	0.24	-	-
$N = 3$	0.72	0.19	0.09	-
$N = 4$	0.46	0.41	0.08	0.05

For three transmitters the APT of a mobile single receiver is expressed as:

$$\bar{t}_{13} = \bar{t}_{p11}\frac{A_{13}}{A_{3t}} + \bar{t}_{p12}\frac{A_{23}}{A_{3t}} + \bar{t}_{p13}\frac{A_{33}}{A_{3t}} \tag{32}$$

where $\bar{t}_{13}$ is the APT of a system with one receiver and three transmitters, $\bar{t}_{pmn}$, A_{nN} and A_{Nt} are as earlier defined. As the number of transmitters increase, the expression of the APT for a mobile single receiver system with N transmitters can be written as:

$$\bar{t}_{1N} = \bar{t}_{p11}\frac{A_{1N}}{A_{3t}} + \bar{t}_{p12}\frac{A_{2N}}{A_{3t}} + ... + \bar{t}_{p1N}\frac{A_{nN}}{A_{Nt}} \tag{33}$$

which is expressed in closed form as:

$$\bar{t}_{1N} = \sum_{n=1}^{N} \bar{t}_{p1n}\frac{A_{nN}}{A_{Nt}} \tag{34}$$

IV. Multiple Receivers

A multiple receiver based IPS uses more than one receiver in the localization of an object. The system can either be designed to receive data from a single LED transmitter or multiple LED transmitters as illustrated in Fig. 8 [24]–[26]. The receivers can be embedded together on a single surface as presented in [24], [26] or distributed over multiple surfaces [27]. Embedded multiple receiver IPS are usually used when the positioning is dependent on a signal parameter such as RSS, AoA or ToA. It involves the use of comparative signal properties. The use of multiple optical receivers with comparable angle of signal arrival or time of signal arrival has been used to improve the positioning accuracy of a LED-based IPS [24]. These methods add to the complexity of such positioning systems and make them less applicable to real life scenarios given practical constraints such as receiver size and power consumption. The embedded receivers have the advantage of maintained geometry such that when there is a shift in the position of one of the receivers, all receivers are equally affected. This is necessary so as to ensure that the mathematical algorithms used for positioning do not break down. The drawback of this system is that a minimum separation in distance is required between the individual receivers and this means an increase in overall receiver size. This system is, therefore, unsuitable to wear and current designs are restricted to bench-tops.

In distributed multiple receivers, each receiver can assume any position, tilt or orientation independently of another. This flexibility in distributed multiple receivers design is because positioning is done by the received signal content as seen in proximity-based indoor positioning. Unlike embedded multiple receivers, distributed receivers give high flexibility of use in positioning and make the device wearable.

This article has been accepted for publication in a future issue of this journal, but has not been fully edited. Content may change prior to final publication. Citation information: DOI 10.1109/ACCESS.2018.2801626, IEEE Access

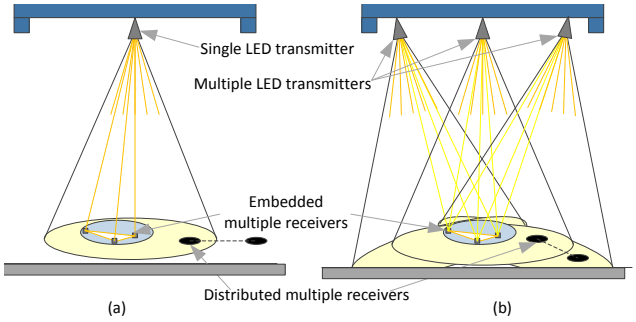

Fig. 8: Illustration of embedded and distributed multiple receivers for (a) single LED transmitter and (b)multiple LED transmitters

Multiple receivers have been proven to improve wireless communication quality and data-rates by the use of the MIMO architecture [28]. In positioning, multiple receivers also increase positioning accuracy by receiving data from additional reference receiver (see Section IV-A). The use of multiple receivers in proximity-based positioning systems, in addition to increasing accuracy, adopts a simple protocol and hardware architecture as described in [29]. This simple architecture transmits data in packets at low bit rates and long distances that are expected in indoor environments. In subsequent sections, we study the effect of distributed multiple receivers on positioning error and positioning time in non-overlapping and multiple overlapping regions as illustrated in Fig. 8(a) and Fig. 8(b) respectively.

A. Motivation behind having an additional receiver

To show how multiple receivers improve positioning error, an intuitive explanation is given and a preliminary simulation is carried out for the transmitter systems under consideration as presented in Fig. 7. For a single receiver in the system of two LED transmitters of Fig. 7, only three unique positions are identifiable: first is when the receiver is in the region of only the first LED, then the region of both the first and second LED and third is when the receiver is in the region of the second LED only. However, by adding an extra receiver with a non-zero distance between the two receivers, five unique positions are identifiable. First is when both receivers are in the region of the first LED, second is when one receiver is in the region of only the first LED and the other receiver is in the region of the overlap between both LEDs, third is when both receivers are in the region of overlap between the two LEDs, fourth is when one receiver is in the region of overlap and the other is in the region of the second receiver only and the fifth position occurs when both receivers are in the region of the second LED. By increasing the number of identifiable regions from 3 to 5 by having an additional receiver, the two-receiver system reduces the positioning error. The simulation compares a single receiver in a two, three and four LED transmitter system with two receivers in the same system. Two Monte-Carlo simulations are carried out to illustrate the advantage of multiple receivers in terms of positioning error. First is a plot of minimum positioning error as the separation between LEDs is increased from 0 m to 1500 mm. If one of the receivers gets positioning data (x_1, y_1) from a LED at location (x_1, y_1) and the other receiver gets data (x_2, y_2) from a LED at location (x_2, y_2), then the estimated position of the receiver for the jth iteration (x_j, y_j) is computed using $x_j = \frac{x_1+x_2}{2}$, and $y_j = \frac{y_1+y_2}{2}$. Given the original position of the receiver is (x_r, y_r), then for a beam radius r, the positioning error is computed as

$$e(r) = \frac{1}{N_i}\sum_{j=1}^{N_i}\sqrt{(x_r - x_j)^2 + (y_r - y_j)^2} \tag{35}$$

where the number of iterations for the simulation is $N_i = 100000$. The error vector $\mathbf{e}$ is the vector of $e(r)$ for r=$[1, 2, ..., 5000]$ mm. The minimum positioning error e_m is given as:

$$e_m = \min(\mathbf{e}) \tag{36}$$

A plot of minimum positioning error as separation between the receivers is increased from 1 to 1500 mm is presented in Fig. 9. Second, is the plot of positioning error using (35) and presented in Fig. 10 at a separation between the two receivers of 500 mm which is an approximate value of the human breadth [30]. The cumulative probability of positioning errors is illustrated in Fig. 11.

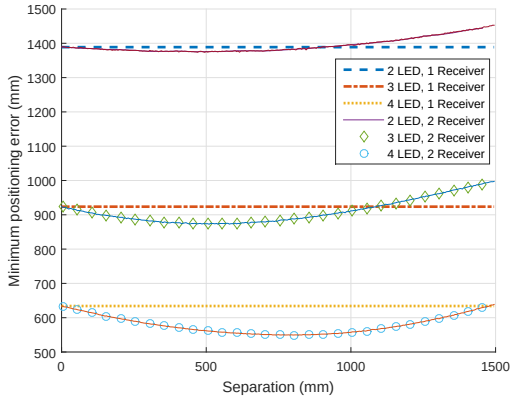

Fig. 9: The effect of separation distance between receivers on positioning error in a two receiver positioning system using the setup in Fig. 7

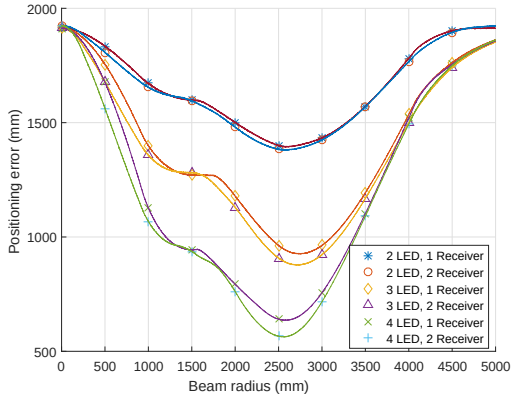

Fig. 10: Positioning improvement by use of two receivers for a system with 2, 3 and 4 LEDs as described in Fig. 7

This article has been accepted for publication in a future issue of this journal, but has not been fully edited. Content may change prior to final publication. Citation information: DOI 10.1109/ACCESS.2018.2801626, IEEE Access

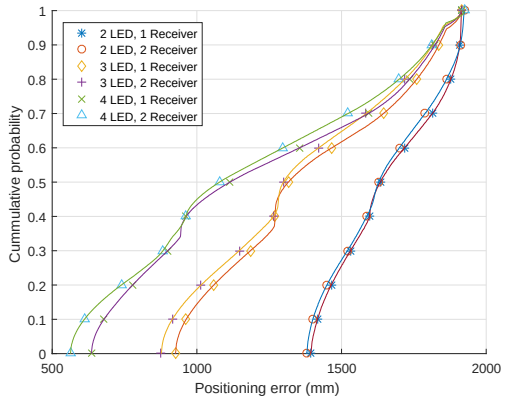

Fig. 11: Cumulative distribution function (CDF) showing the cumulative probability spread of positioning error for the setup described in Fig. 7

Based on Fig. 9, Fig. 10 and Fig. 11, the properties of a two receiver system can be written as follows:

a. At 0 separation between receivers, the two-receiver system behaves just like a single receiver system.
b. The U-curves in both plots show that optimal values of separation and beam radius, which is the radius of the circular footprint formed by an LED on a horizontal plane, can be selected for reduction in positioning errors for a two-receiver system.
c. At constant separation of 500 mm between the receivers, a two receiver system shows reduction of error in a two transmitter system by 1.1%, in three transmitter system the reduction is 5.5% and in a four transmitter system, it is 11.5%. Therefore, increasing the number of LED transmitters from 2 to 4 increases the reduction in positioning error for the two receiver system.
d. The CDF shows that the use of a two receiver system can reduce positioning error in a room to about 56 cm and this value can be further reduced for separation around 75 cm in a four LED transmitter system.

Having demonstrated how multiple receivers reduce positioning error, in the rest of this work, we quantify the effect of positioning time for the hardware-friendly PDM collision handling algorithm. By increasing the number of transmitters and receivers in order to improve positioning accuracy, the positioning time is estimated and actual results are presented in Section VI.

V. Multiple Receiver Positioning Time

Depending on the number of transmitters considered, a receiver can either be in a region of one LED light, a region of two, three, or four overlaps. To determine the positioning time of a multiple receiver system, given the positioning time of a receiver in any overlap region, the multiple receiver positioning time is equal to the positioning time of any of the receivers in the region of the highest number of overlap among other receivers. Considering a scenario of two transmitters and two receivers, if both receivers are in a region of one LED (with no overlap), the positioning time is the time when a single receiver is in this region. However, if one of the receivers is in a position of two overlaps, the positioning time is that of a single receiver in a region of two overlaps. To determine the positioning time for multiple receivers in this system two analytic processes are considered. First is the positioning time of a stationary multiple receiver system and then, the positioning time of a mobile multiple receiver system.

A. APT for stationary multiple receiver system

The APT for a stationary multiple receiver system is dependent on the probability that a receiver in a N transmitter system is in either a one LED, two overlap, three overlap or up to N overlaps. To determine the APT, an expression for the probability that a receiver's positioning time is defined by n overlaps in a N transmitter system is first developed and then this expression is used to compute the APT.

1) Probability that a receiver's positioning time is defined by specific overlap region: Considering a system with two transmitters and two receivers, any of these receivers can only be in either one LED or two LED overlap region. Table III lists the possible receiver positions. In each scenario, the receiver R_d that determines the positioning time is the receiver in a region of the highest number of overlaps. To ensure all receivers can be in all region of overlaps, the maximum separation between two receivers is kept below 500 mm as presented in Section IV-A. Table IV and Table V shows the values of R_d for a two receiver system with three and four transmitters respectively.

TABLE III: Possible receiver location for 2 receivers Rx_1, Rx_2 and two transmitters

Rx_1	Rx_2	R_d
1	1	1
1	2	2
2	1	2
2	2	2

TABLE IV: Possible receiver location for 2 receivers Rx_1, Rx_2 and three transmitters

Rx_1	Rx_2	R_d
1	1	1
1	2	2
1	3	3
2	1	2
2	2	2
2	3	3
3	1	3
3	2	3
3	3	3

By the values of R_d is Table III, the probability that the APT is determined by the positioning time of receivers in one LED region is one out of four possibilities and the probability that the APT is determined by the APT of receivers in the two overlap region is three out of four possibilities. If $P_{rN}(n)$ is the probability that the APT in a r receiver system with N transmitters is determined by n number of overlaps, from Table III, we can write $P_{22}(1) = 0.25$ and $P_{22}(2) = 0.75$. For a three transmitter system, from Table IV, we can write

This article has been accepted for publication in a future issue of this journal, but has not been fully edited. Content may change prior to final publication. Citation information: DOI 10.1109/ACCESS.2018.2801626, IEEE Access

TABLE V: Possible receiver location for 2 receivers Rx_1, Rx_2 and four transmitters

Rx_1	Rx_2	R_d
1	1	1
1	2	2
1	3	3
1	4	4
2	1	2
2	2	2
2	3	3
2	4	4
3	1	3
3	2	3
3	3	3
3	4	4
4	1	4
4	2	4
4	3	4
4	4	4

$P_{23}(1) = \frac{1}{9}$, $P_{23}(2) = \frac{3}{9}$ and $P_{23}(3) = \frac{5}{9}$. From Table V, the probabilities that the APT is determined by $1, 2, 3$ or 4 overlaps are $P_{24}(1) = 0.0625$, $P_{24}(2) = 0.1875$,$P_{24}(3) = 0.3125$ and $P_{24}(4) = 0.4375$ respectively. By observing this series, a general expression for these probabilities can be written as:

$$P_{2N}(n) = \frac{2n-1}{N^2} \tag{37}$$

For r receivers, the probability $P_{rN}(n)$ can be written as:

$$P_{rN}(n) = \frac{n^r - (n-1)^r}{N^r} \tag{38}$$

(see proof in Appendix B)

2) APT expression for stationary multiple receiver IPS: In this section, the average positioning for a stationary multiple receiver system is derived using the probability expressions derived in Section V-A1. Considering a region of two transmitters and two receivers, the positioning time can either be determined by the positioning time in a region of two overlaps or the positioning time in a region of one LED. Therefore the APT for stationary multiple receiver can be written as:

$$\bar{t}_{s22} = \bar{t}_{p11}P_{22}(1) + \bar{t}_{p12}P_{22}(2). \tag{39}$$

For a system with two receivers and three transmitters, the APT is written as:

$$\bar{t}_{s23}\bar{t}_{p11}P_{23}(1) + \bar{t}_{p12}P_{23}(2) + \bar{t}_{p13}P_{23}(3) \tag{40}$$

where $\bar{t}_{srN}$ is the APT for a r stationary multiple receiver system with N transmitters. A general expression for a two multiple receiver system with N transmitters could therefore be expressed as:

$$\bar{t}_{s2N} = \sum_{n=1}^{N} P_{2N}(n)\bar{t}_{p1n} \tag{41}$$

Extending (41) to r multiple receivers, the APT can be written as:

$$\bar{t}_{srN} = \sum_{n=1}^{N} P_{rN}(n)\bar{t}_{p1n} \tag{42}$$

By substituting (38) into (42), the APT $\bar{t}_{srN}$ for r stationary multiple receivers in a system of N overlapping transmitters can be written as:

$$\bar{t}_{srN} = \frac{1}{N^r}\sum_{n=1}^{N}(n^r - (n-1)^r)\bar{t}_{p1n} \tag{43}$$

B. APT for a mobile multiple receiver system

Two probabilities that determine the APT for a mobile multiple receiver system are the probability that the receiver is in a specific region of overlap and the probability that the positioning time is defined by a certain number of overlaps. The probability that the positioning time is defined by a certain number of overlaps is derived in Section V-A1 of this work and the probabilities that a receiver is in a specific region is the ratio of the area of that region to the total area covered by the LED transmitters in the system. Considering the system in Fig. 7, the areas covered by all possible number of overlap regions have been estimated in Table II. Let the probability that a mobile multiple receiver system is in a region of n overlaps in a system of N LED transmitters $P_{aN}(n)$ be expressed as $\frac{A_{nN}}{A_{Nt}}$. Considering a two LED overlap system with two receivers, if the probability that the receivers are in a region of one LED is represented as $P_{a2}(1)$ and the probability that the receivers are in a region of two LED overlap is $P_{a2}(2)$. From the values of $\frac{A_{nN}}{A_{Nt}}$ in Section III-D, $P_{a2}(1) = \frac{A_{12}}{A_{2t}}$, $P_{a2}(2) = \frac{A_{22}}{A_{2t}}$. The probability that the positioning time is defined by a region of one LED is defined in Section V-A1 as $P_{22}(1)$ and $P_{22}(2)$ is the probability that the positioning time of a region is defined by two LEDs.

For this system, both receivers can either be in a region of one LED only and the positioning time is based on the time in this region or any of the receivers are in a region of two LED overlap and the positioning time is based on the two overlap region. It is not possible that both receivers are in a one LED only and the positioning time is determined by the two overlap region neither is it possible that any or both of the receivers are in a region of two LED overlap and the positioning time is determined by the one LED only region. Consequently, the probability that both receivers are in a region of one LED can be written as $\frac{P_{a2}(1)P_{22}(1)}{P_{a2}(1)P_{22}(1)+P_{a2}(2)P_{22}(2)}$ and the probability that the receiver is in a two LED overlap region is $\frac{P_{a2}(2)P_{22}(2)}{P_{a2}(1)P_{22}(1)+P_{a2}(2)P_{22}(2)}$. The APT for a mobile multiple receiver system in a two receiver, two transmitter system $\bar{t}_{m22}$ can, therefore, be written as:

$$\bar{t}_{m22} = \frac{P_{a2}(1)P_{22}(1)}{P_{a2}(1)P_{22}(1) + P_{a2}(2)P_{22}(2)}\bar{t}_{p11} + \frac{P_{a2}(2)P_{22}(2)}{P_{a2}(1)P_{22}(1) + P_{a2}(2)P_{22}(2)}\bar{t}_{p12} \tag{44}$$

For two receivers and three transmitters, by a similar argument, the APT can be written as:

$$\bar{t}_{m23} = \frac{P_{a3}(1)P_{23}(1)\bar{t}_{p11} + P_{a3}(2)P_{23}(2)\bar{t}_{p12}}{P_{a3}(1)P_{23}(1) + P_{a3}(2)P_{23}(2) + P_{a3}(3)P_{23}(3)} + \frac{P_{a3}(3)P_{23}(3)\bar{t}_{p13}}{P_{a3}(1)P_{23}(1) + P_{a3}(2)P_{23}(2) + P_{a3}(3)P_{23}(3)} \tag{45}$$

This article has been accepted for publication in a future issue of this journal, but has not been fully edited. Content may change prior to final publication. Citation information: DOI 10.1109/ACCESS.2018.2801626, IEEE Access

In general, for N transmitters and r receivers, the APT for a mobile multiple receiver system can be written as:

$$\bar{t}_{mrN} = \frac{\sum_{n=1}^{N} P_{aN}(n) P_{rN}(n) \bar{t}_{p1n}}{\sum_{i=1}^{N} P_{aN}(i) P_{rN}(i)} \tag{46}$$

VI. Results and Discussions

In this section, results for the probability of collision are verified by simulations and the results for the positioning times for the different designs are presented.

A. Probability of collision

The communication toolbox in the MATLAB® software package is used to present the probability of collision 2, 3 and 4 overlap regions. The simulated probability of collision, calculated as the ratio of collided packets to the total number of packets sent, is presented for varying cycle time t_c between 0 and 400 ms. The process is repeated for all scenarios considered in Section III of this work. For the synchronized and the semi-synchronized systems, the probability of collision is always zero and therefore not shown.

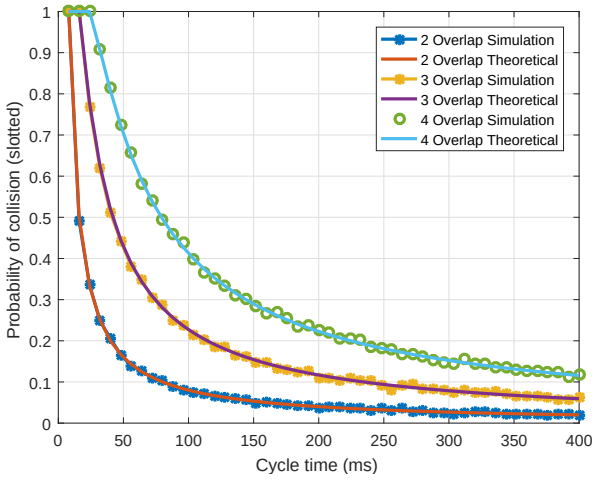

Fig. 12: Simulation and mathematical model of probability of collision P_{csN} in (12) for $N = 2$, $N = 3$ and $N = 4$ overlap slotted unsynchronized system representing region **b**, **c** and **d** of Fig. 1b vs cycle time t_c

For the slotted unsynchronized system, Fig. 12 shows the relationship between probability of collision and varying cycle times for 2-overlap, 3-overlap, and 4-overlap regions between 0 and 400 ms. In Fig. 12, the mathematical model is also compared with software-based simulations of the probability of collision at the receiver and the results show that the mathematical models represent the system correctly. In addition, it is observed from Fig. 12 that the probability of collision for a particular cycle time increases with increase in the number of LEDs in the overlap region. The rate of decrease of the probability of collision as the cycle time increases is also faster for lower number of LEDs in a region.

The unslotted unsynchronized system simulation results are presented in Fig. 13 for region **b**, region **c**, and region **d**. Suffice it to say no overlap occurs at region **a** so it is not considered here. Fig. 13 shows that unslotted unsynchronized systems generally have similar decay curve to that of the slotted unsynchronized system and in addition, like the slotted system, the probability of collision decrease with increase in the cycle time.

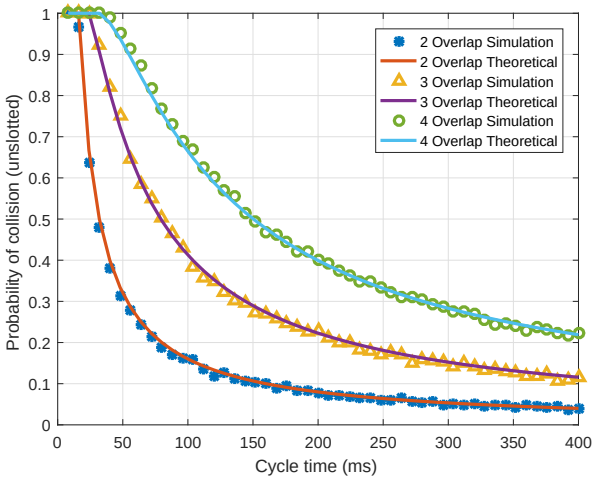

Fig. 13: Simulation and mathematical model of probability of collision P_{cuN} in (24) for $N = 2$, $N = 3$ and $N = 4$ overlap unslotted unsynchronized model representing region **b**, **c** and **d** of Fig. 1b vs cycle time t_c

The unslotted system, however, shows a probability of collision that approximately doubles the value in a slotted unsynchronized system if all other parameters are equal. For both systems (slotted unsynchronized and unslotted unsynchronized), the minimum value for the cycle time is the product of the packet time and number of LED transmitters considered. If this value is not greater than the number of LEDs in the region, Fig. 13 shows that the probability of collision is maintained at 1. This implies there will not be any successful data transmission and therefore no positioning.

B. Positioning time

In this section, the APTs for the systems considered in this work are simulated and the results are presented. For consistency, the APT is plotted against the cycle time for all the designs considered in this paper. The positioning times for both the synchronized system and the semi-synchronized system, represented by (4) and (6), are equal for equal packet sizes. The positioning times for these systems are also independent of the cycle time as they only depend on the number of LEDs in the region and the packet time.

Since packet time is dependent on the protocol used for transmission, to observe general patterns, packet time is assumed to be 8 ms in this paper. The APT plot for the slotted unsynchronized system with varying number of overlaps is shown in Fig. 14. The curves in Fig. 14 show a fast fall in positioning time then a slow rise as cycle time increases. The curves imply that at low cycle times, the APT is high due to packets lost in collision as the probability of collision is high in the low cycle time interval. At high cycle time, the APT is high due primarily to slow rate of arrival of packets.

This article has been accepted for publication in a future issue of this journal, but has not been fully edited. Content may change prior to final publication. Citation information: DOI 10.1109/ACCESS.2018.2801626, IEEE Access

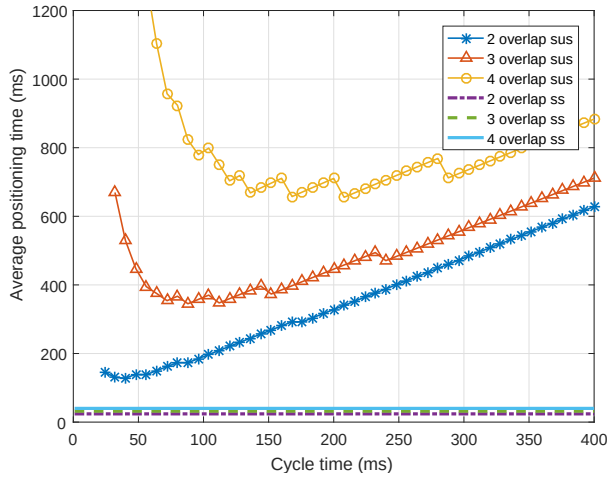

Fig. 14: Average position time variation with cycle time t_c for slotted unsynchronized system (sus) $\bar{t}_{ps}$ from (19) compared with the synchronized system (ss) t_{pN} for 2, 3, and 4 overlaps

Between the two extremes are points of reduced and optimal APT. Based on Fig. 14, the system can be designed to operate at an APT of approximately 650 ms with as much as four LEDs in the overlap region.

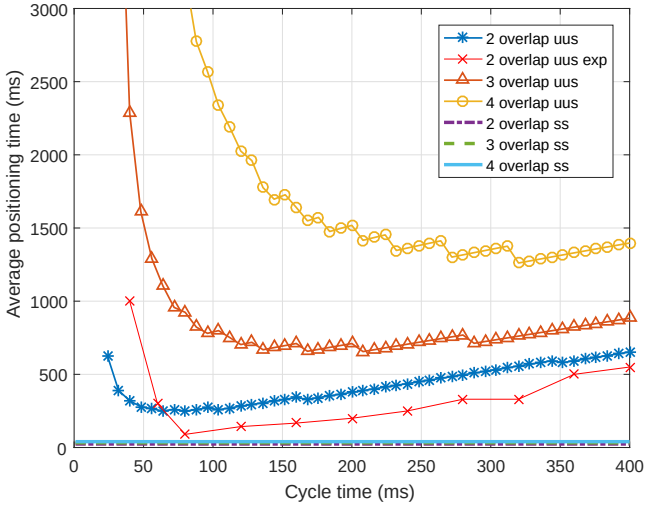

Fig. 15: Average position time variation with cycle time t_c for unslotted unsynchronized system (uus) $\bar{t}_{pu}$ from (29) compared with the synchronized system (ss) t_{pN} for 2, 3, and 4 overlaps and experimental (exp) 2 overlap system

The APT plot for the unslotted unsynchronized system is presented in Fig. 15. The APT for this system is higher than the time for positioning of the slotted unsynchronized system. However, at high duty cycles, both systems tend to have similar APT. The APT of this system can be designed to be as low as 250 ms in region of 2 overlaps and about 1300 ms in a region of 4 overlaps. For practical applications, if positioning is required every second, Fig. 14 shows that cycle time could be kept between 70 and about 400 ms for the slotted unsynchronized system and from Fig. 15, the cycle time could be kept between 120 and about 400 ms for the unslotted unsynchronized system APT to be kept below 2 s. These ranges show that positioning can be received every two seconds and therefore the IPS can be used to monitor stationary objects. This wide range of cycle time for satisfactory positioning also allows for flexibility in design and also the incorporation of effects such as light dimming while positioning.

1) Experimental validation: In order to validate the APT, the unslotted unsynchronized system using 2 LED transmitters and one receiver is implemented in hardware using ATMEG 328 microcontrollers. The experimental setup consists of a PC that is used to program the microcontroller for each transmitter at increasing cycle times as shown in Fig. 16. Both transmitters and the receiver are powered from the power supply unit through the electronic unit which consists of the ATMEG 328 microcontrollers and a transistor-based driver circuitry. The packets transmitted from the LEDs arrive at the receiver and are decoded by the receiver microcontroller. The time taken to receive two correctly decoded packets from both transmitters is measured as the positioning time. This is repeated five times and the APT is computed as the average of the five values. This APT is plotted as the two overlap unslotted unsynchronized system experiment in Fig. 15.

The curves in Fig. 15 show the experimental results have the same pattern as the analytical APT for 2 overlap unslotted unsynchronized system. However, the experimental system has lower APT for cycle time values greater than 70 ms. This is because the analytical results guarantees a 99.99% success rate so this represents a worst case timing scenario when the probability of collision is low. A match between experimental measurements and the analytical system is observed at a cycle time of 70 ms and the curve shows that as the cycle time increases towards 400 ms, the deviation between the experimental results and the simulation result reduces. Based on the experimental results, the unslotted unsynchronized system for two LEDs gives an APT of 100 ms when the cycle time is selected to be 80 ms.

C. Mobile single receiver system

Here the analytical results of the positioning times for a moving receiver are presented for a synchronized system, unsynchronized system, slotted unsynchronized system, and unslotted unsynchronized system. The APT is derived by increasing cycle time from (19) and (29) and by substituting the values of other variables in (34).

The APT for a mobile single receiver system with two, three and four transmitters are presented in Fig. 17. This plot gives three important information about the positioning time of a single receiver system. First, the curves in Fig. 17 reveal that at high duty cycles, the difference in APT between the slotted unsynchronized system and the unslotted unsynchronized system is lower than 100 ms. This means that the unslotted unsynchronized system, which is easier to implement, can be used in place of the slotted unsynchronized system without much sacrifice in APT. Secondly, Fig. 17 shows that for a system with up to 4 LEDs overlap, the APT is below 1 ms. Although, in a 4 overlap region Fig. 15 has

This article has been accepted for publication in a future issue of this journal, but has not been fully edited. Content may change prior to final publication. Citation information: DOI 10.1109/ACCESS.2018.2801626, IEEE Access

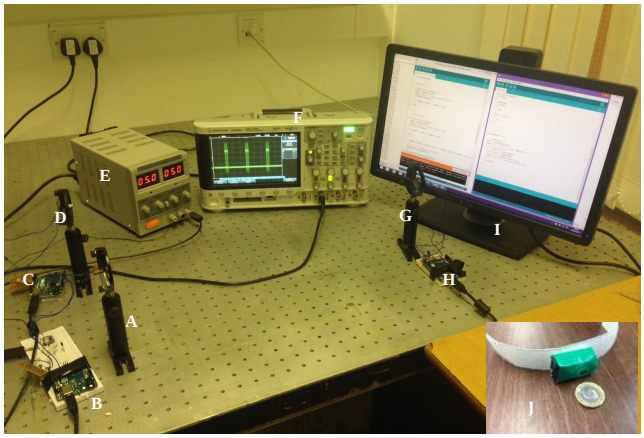

Fig. 16: Experimental setup. A: transmitter 1, B: transmitter 1 electronic unit, C: transmitter 2 electronic unit, D: transmitter 2, E: power supply unit, F: digital oscilloscope, G: receiver, H: receiver electronic unit, I: PC showing monitor for programming and serial port monitoring, J: Inset of wearable receiver prototype

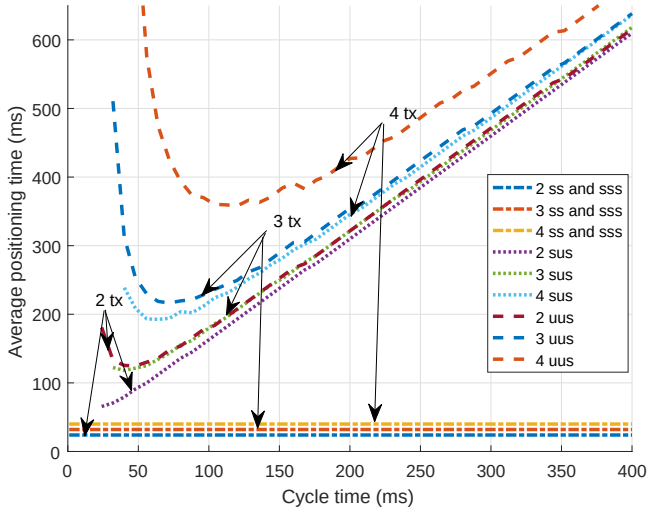

Fig. 17: Average position time $\bar{t}_{1N}$ in (34) vs cycle time t_c for a mobile single receiver where ss:synchronized system, sss:semi-synchronized system, sus:slotted unsynchronized system and uus:unslotted unsynchronized system

shown that the APT is about 1 s, but due to the small area covered by this region as shown in Fig. 7, the overall APT for a mobile receiver averages at about half a second when the cycle time is designed to be about 250 ms. Thirdly, from the curves in Fig. 17, the APT shows minimum points, which can be used to design an overall positioning system, of about 370 ms for the unslotted unsynchronized system and about 200 for the slotted unsynchronized system.

D. Stationary multiple receiver system

In this section, the results of performance of stationary multiple receiver systems are presented. Slotted synchronized system and unslotted synchronized systems are considered and presented in Fig. 18 and Fig. 19 respectively.

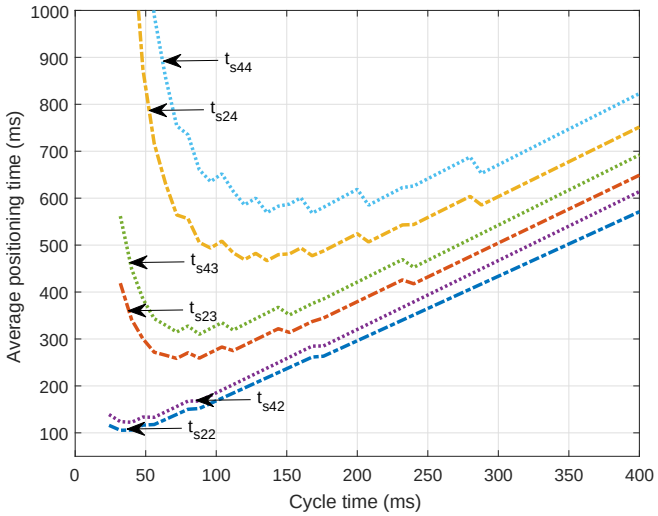

Fig. 18: Average position time $\bar{t}_{srN}$ in (43) vs cycle time t_c for stationary multiple receivers in slotted unsynchronized multiple transmitter overlap region where t_{srN} represents the APT for r receivers and N transmitters

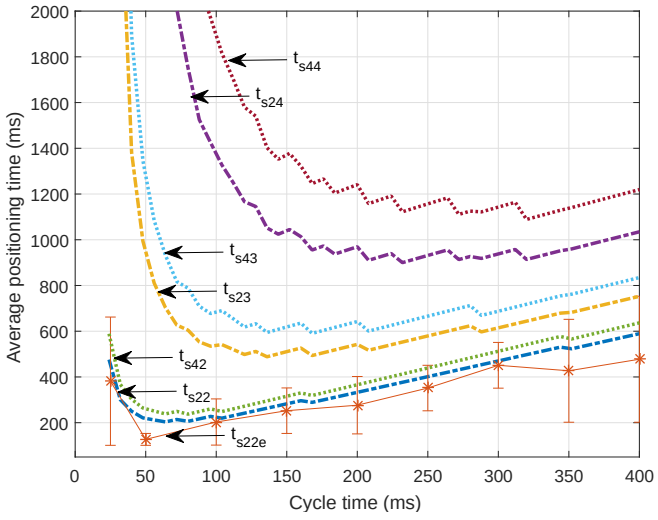

Fig. 19: Average position time $\bar{t}_{srN}$ in (43) vs cycle time t_c for stationary multiple receivers in unslotted unsynchronized multiple transmitter overlap region where t_{srN} represents the APT for r receivers and N transmitters. t_{s22e}: Experimental result

For a slotted unsynchronized system, Fig. 18 shows that the APT is influenced more by the number of transmitters than the number of receivers. For two transmitters, as the number of receivers are increased, the APT increases by about 10 ms. However, for two receivers the APT increases by about 100 ms for 100 ms cycle time as the number of transmitters are increased from 2 to 4. As the cycle time increases, the effect of an increase in transmitters or receiver reduces. This is seen as the lines of the curves converge as cycle time approaches 400 ms.

The APT plots for unslotted unsynchronized systems presented in Fig. 19 also show that the number of transmitters is the major determinant of the APT in similar manner to the

This article has been accepted for publication in a future issue of this journal, but has not been fully edited. Content may change prior to final publication. Citation information: DOI 10.1109/ACCESS.2018.2801626, IEEE Access

slotted synchronized system. The APT curves fall then rises and the range of cycle time between a fall and a rise is seen to increase as the number of transmitters increases. Therefore, the range of minimum cycle times for two transmitters is smallest, and the range is larger for four transmitters and increases as the number of transmitters increase. The minimum APT for a two transmitter system is about 200 ms and this occurs at a cycle time between 50 and 75 ms. For a three transmitter system, it is about 500 ms and this occurs at a cycle time about the range 125 - 175 ms. The minimum APT for the four transmitter system is about 900 ms and this occurs at a cycle time within the range 150 and 375 ms.

Experiments to test the performance of a two-receiver system using the same setup as described in Section VI-B1 with the single receiver changed to a multiple receiver system with two receivers. The APT measured with the device is presented in Fig. 19. Unlike the single receiver system, the APT for the two receiver system shows error bars which indicate the average of the plots at each point, the maximum and the minimum APT. This is because the flexibility of the two receiver system allows positioning when data is received from one receiver and packet collision occurs at the other receiver. In this case, the system behaves as if the receiver where collision occurs is blocked from light thereby giving a position in a short time. However, in experimental measurements, it is ensured that the average of correct APTs when both receivers received packets successfully are measured and this is plotted in Fig. 19.

E. Mobile multiple receiver system

When the receiver moves in a room of two, three or four LED transmitter with orientation as described in Fig. 7, the overall APT for two and four multiple receivers in slotted unsynchronized and unslotted unsynchronized systems is presented in Fig. 20 and Fig. 21 respectively.

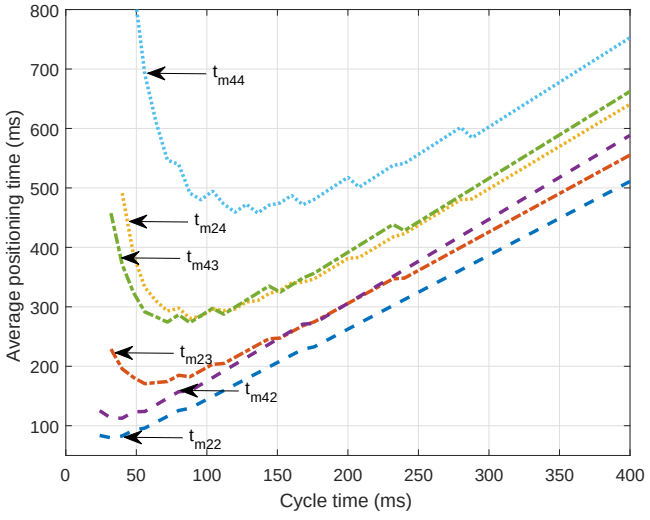

Fig. 20: Average position time $\bar{t}_{mrN}$ in (46) vs cycle time t_c for mobile multiple receivers in slotted unsynchronized multiple transmitter overlap region where t_{mrN} represents the APT for r receivers and N transmitters

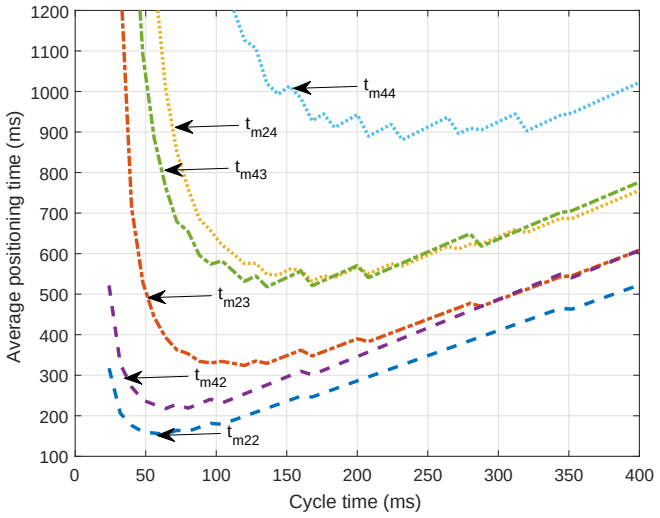

Fig. 21: Average position time $\bar{t}_{mrN}$ in (46) vs cycle time t_c for multiple receivers in unslotted unsynchronized multiple transmitter overlap region where t_{mrN} represents the APT for r receivers and N transmitters

When a multiple receiver system is static, the APT for up to four transmitters is about 1 s as seen in Fig. 18 and Fig. 19. However, when a person is moving around across different overlap regions in a room, the APT, shown in Fig. 20 and Fig. 21 for slotted and unslotted unsynchronized systems, is observed to stay below a second when the cycle time is between 150 and 350 ms. For two receivers, the positioning time is about 300 ms for the slotted system and 550 ms for unslotted system.

VII. Conclusions and Future Work

In this paper, we discuss, design and analyse practical installation techniques that could be used to implement the MLEM-based IPS design using inexpensive off-the-shelf hardware. Three practical designs for the implementation of MLEM indoor positioning system are considered. The designs include a synchronized system, a semi-synchronized system and unsynchronized systems. The synchronized system has the best performance in terms of positioning time but it requires a redesign of existing lighting facilities. The semi-synchronized system with similar positioning time as the synchronized system offers a more practical implementation but requires each LED to be tagged with a specific delay. To avoid these complexities, we designed PDM collision-handling algorithms that allow for use of unsynchronized LEDs in positioning. The unsynchronized systems spread packets in a low duty cycle and collisions are reduced by increasing cycle time. The unsynchronized systems are designed to be simple as they do not require any coordination. The probabilities of collision for the unsynchronized system are computed analytically and the developed analytical expressions are verified by extensive Monte-Carlo simulations. This paper also shows that the accuracy of the MLEM system is improved by the use of multiple receivers. The IPS gives a sub-meter positioning error in a standard room of dimension 5 m $\times$ 5 m $\times$ 3 m.

This article has been accepted for publication in a future issue of this journal, but has not been fully edited. Content may change prior to final publication. Citation information: DOI 10.1109/ACCESS.2018.2801626, IEEE Access

The performances of the systems are evaluated by computing the positioning time. Based on the simple hardware implementation approach used, the positioning time increases for an increase in the number of transmitters and receivers. The results show that careful selection of the cycle time is necessary to keep the positioning time low. For slotted unsynchronized systems, the APT is below half a second and for unslotted unsynchronized systems, it is below 1 s. The analytical results of the positioning time for two transmitter and single and two receivers systems are validated by experimental measurement of built prototypes. In terms of performance, for a mobile receiver, all systems are shown to have APTs that are below a second which is good for human positioning. Multiple receiver designs not only increases positioning accuracy but also improves the robustness of the MLEM IPS because if one of the receivers is blocked or does not receive a LOS signal, positioning can be achieved from the other receivers.

Conclusively, this paper introduced novel unsynchronized designs for collision handling in proximity-based positioning. Analytical results are developed which match simulations and experiment. The prototype of the design is inexpensive, lightweight, wearable and not totally dependent on line of sight. Future work will study the robustness of the designed IPS in terms of tilted receivers.

APPENDIX A
DERIVATION OF RATIOS OF AREAS OF OVERLAPS IN PRESENTED IN TABLE 2

Here we show how to derive the ratios of areas of various overlap regions. For two overlapping circles with equal radii, by circle geometry, the area of overlap A_{22} is known to be:

$$A_{22} = 2r^2 \cos^{-1} \frac{\mathfrak{d}}{2r} - \frac{\mathfrak{d}}{2}\sqrt{4r^2 - \mathfrak{d}^2} \tag{A.47}$$

where $\mathfrak{d}$ is the distance between the centers of the two circles and r is the radius of any of the circles. The total area of the overlapped circles is $A_{2t} = 2\pi r^2 - A_{22}$ and the area of non-overlapping regions $A_{12} = A_{2t} - A_{22}$. Although no generic formulae exists for calculating all areas of overlapping region for more than two overlapping circles, calculating these areas follow basic rules of circle geometry. For three overlapping circles as shown in Fig. A.22, the area of $\triangle$ABC is calculated from the known sides. The area of the three overlap region A_{33} is calculated as the sum of the area of $\triangle$ABC and $3\times$(Area of sector ABEC - $\triangle$ABC). Area of two overlap only A_{23} can be calculated as $3\times$ area of ABCD - A_{33} where area of ABCD is the area of two overlapping circles as given in (A.47). The area of only one circle can be calculated as the area of ABCD + $A_{23}/3$ subtracted from the area of each circle. The same argument is used to estimate area of overlapping regions for four circles and the results presented in Table II.

APPENDIX B
PROOF FOR PROBABILITY THAT A RECEIVER'S POSITIONING TIME IS DEFINED BY A SPECIFIC OVERLAP REGION

In this appendix, we present proofs for the probability that a receiver's positioning time is defined by a specific overlap region as described in (37) and (38). To prove these equations, we use multidimensional mathematical induction (MI). Since (38) is the rth term of (37), two-dimensional MI is used to prove (37), then by multidimensional MI, (37) this is used as a base case of a sequence to give proof of (38).

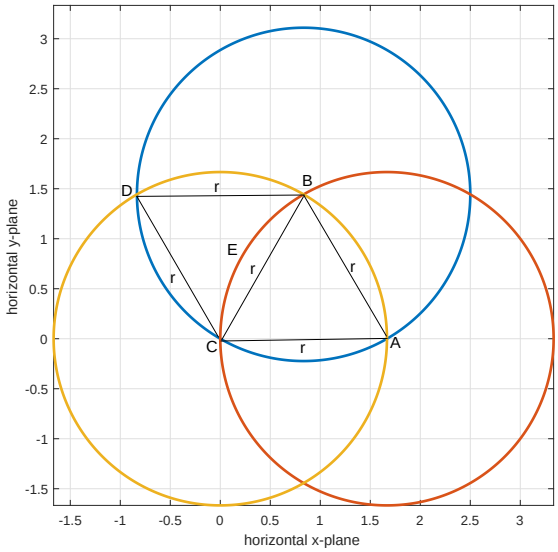

Fig. A.22: Illustration of overlap between 3 circles used to determine the overlap areas

Proposition for (37)*::* The probabilities that a 2-receiver is in an area of n overlap in a N number of transmitter system given by Table B.6 can be represented as:

$$P_{2N}(n) = \frac{n^2 - (n-1)^2}{N^2} = \frac{2n-1}{N^2}, \qquad 1 \le n \le N. \tag{B.48}$$

TABLE B.6: Probability that a 2-receiver in N transmitter system is in m number of overlaps region

$P_{2N}(n)$	$n=1$	$n=2$	$n=3$	$n=4$
$N=2$	$\frac{1}{4}$	$\frac{3}{4}$	-	-
$N=3$	$\frac{1}{9}$	$\frac{3}{9}$	$\frac{5}{9}$	-
$N=4$	$\frac{1}{16}$	$\frac{3}{16}$	$\frac{5}{16}$	$\frac{7}{16}$

Proof: Base case: $P_{22}(1) = \frac{1}{4}$. Induction over N: assuming $P_{2k}(1)$ is true. From (B.48), $P_{2k}(1) = \frac{1}{k^2}$. If $k = k+1$ this becomes $P_{2(k+1)}(1) = \frac{1}{(k+1)^2}$. By direct evaluation of $P_{2(k+1)}(1)$ where $N = k+1$ from (B.48), we get $P_{2(k+1)}(1) = \frac{1}{(k+1)^2}$. Thus the induction over N for the proposition is true. Induction over n: assuming the proposition holds true for $P_{2q}(k)$ where q is any positive integer representing N as validated by the induction over N. From (B.48), $P_{2q}(k) = \frac{k^2-(k-1)^2}{q^2} = \frac{k^2-(k^2-2k+1)}{q^2} = \frac{2k-1}{q^2}$. If $k = k+1$ this becomes $P_{2q}(k) = \frac{2k+1}{q^2}$. By direct evaluation of $P_{2q}(k+1)$ from (B.48), we get $P_{2q}(k+1) = \frac{(k+1)^2-k^2}{q^2} = \frac{2k+1}{q^2}$. Thus the induction over n for the proposition is also true. By verifying in both dimensions N and n that (B.48) is true for a base case and also true at $k+1$, then, for any positive integer k, (37) is

proven true.

Proposition for (38)*::* The probabilities that a r-receivers are in an area of n overlap in a N number of transmitters system can be represented as:

$$P_{rN}(n) = \frac{n^r - (n-1)^r}{N^r}, \qquad 1 \leq n \leq N. \quad \text{(B.49)}$$

Proof: Base case: $P_{22}(1) = \frac{1}{4}$. Considering the series $P_{2N}(n)$, $P_{3N}(n)$, $P_{4N}(n)$,...,$P_{rN}(n)$, since the induction over N and n has been proven true, for induction over r, assuming $P_{kn}(n)$ is true. From (B.48), $P_{kn}(n) = \frac{n^k-(n-1)^k}{n^k} = 1 - (\frac{n-1}{n})^k$. If $k = k+1$, this becomes $P_{(k+1)n}(n) = 1 - (\frac{n-1}{n})^{k+1} = 1 - (\frac{n-1}{n})(\frac{n-1}{n})^k$. By direct substitution of $k+1$ for k in (B.49), if $n = N$, $P_{(k+1)n}(n) = \frac{n^{k+1}-(n-1)^{k+1}}{n^{k+1}} = 1 - (\frac{n-1}{n})(\frac{n-1}{n})^k$. Thus verifying the induction over r.

Remark: By the use of multidimensional MI, the probability equations that a r number of multiple receivers in a N transmitter system is in a region of n number of overlaps is verified to be true.

ACKNOWLEDGEMENT

This research is supported by the School of Engineering and Built Environment of Glasgow Caledonian University through the University sponsored research studentship.

REFERENCES

[1] R. B. Thompson, "Global positioning system: the mathematics of GPS receivers," *Mathematics magazine*, vol. 71, no. 4, pp. 260–269, 1998.

[2] S. Ingram, D. Harmer, and M. Quinlan, "Ultrawideband indoor positioning systems and their use in emergencies," in *Position Location and Navigation Symposium, 2004. PLANS 2004*. IEEE, 2004, pp. 706–715.

[3] S.-H. Jung, G. Lee, and D. Han, "Methods and tools to construct a global indoor positioning system," *IEEE Transactions on Systems, Man, and Cybernetics: Systems*, 2017.

[4] M. B. Kjærgaard, H. Blunck, T. Godsk, T. Toftkjær, D. L. Christensen, and K. Grønbæk, "Indoor positioning using GPS revisited," in *International conference on pervasive computing*. Springer, 2010, pp. 38–56.

[5] K. Kaemarungsi and P. Krishnamurthy, "Modeling of indoor positioning systems based on location fingerprinting," in *Twenty-third Annual Joint Conference of the IEEE Computer and Communications Societies (INFOCOM)*, vol. 2. IEEE, 7-11 March 2004, pp. 1012–1022.

[6] J. Vongkulbhisal, B. Chantaramolee, Y. Zhao, and W. S. Mohammed, "A fingerprinting-based indoor localization system using intensity modulation of light emitting diodes," *Microwave and Optical Technology Letters*, vol. 54, no. 5, pp. 1218–1227, 2012.

[7] M. Kok, J. D. Hol, and T. B. Schön, "Indoor positioning using ultrawideband and inertial measurements," *IEEE Transactions on Vehicular Technology*, vol. 64, no. 4, pp. 1293–1303, 2015.

[8] N. A. Mohammed and M. A. Elkarim, "Exploring the effect of diffuse reflection on indoor localization systems based on RSSI-VLC," *Optics express*, vol. 23, no. 16, pp. 20 297–20 313, 10 August 2015.

[9] S.-H. Yang, H.-S. Kim, Y.-H. Son, and S.-K. Han, "Three-dimensional visible light indoor localization using AOA and RSS with multiple optical receivers," *Journal of Lightwave Technology*, vol. 32, no. 14, pp. 2480–2485, 15 July 2014.

[10] T.-H. Do and M. Yoo, "TDOA-based indoor positioning using visible light," *Photonic Network Communications*, vol. 27, no. 2, pp. 80–88, 2014.

[11] S. Murata, C. Yara, K. Kaneta, S. Ioroi, and H. Tanaka, "Accurate indoor positioning system using near-ultrasonic sound from a smartphone," in *2014 Eighth International Conference on Next Generation Mobile Apps, Services and Technologies*. IEEE, 2014, pp. 13–18.

[12] J. Blankenbach, A. Norrdine, and H. Hellmers, "Adaptive signal processing for a magnetic indoor positioning system," *Indoor positioning and indoor navigation*, 2011.

[13] B. Lin, X. Tang, Z. Ghassemlooy, C. Lin, and Y. Li, "Experimental demonstration of an indoor vlc positioning system based on ofdma," *IEEE Photonics Journal*, vol. 9, no. 2, pp. 1–9, 2017.

[14] H. Lv, L. Feng, A. Yang, P. Guo, H. Huang, and S. Chen, "High accuracy vlc indoor positioning system with differential detection," *IEEE Photonics Journal*, vol. 9, no. 3, pp. 1–13, 2017.

[15] A. Bekkelien, M. Deriaz, and S. Marchand-Maillet, "Bluetooth indoor positioning," *Master's thesis, University of Geneva*, 2012.

[16] S.-H. Fang, C.-H. Wang, T.-Y. Huang, C.-H. Yang, and Y.-S. Chen, "An enhanced zigbee indoor positioning system with an ensemble approach," *IEEE Communications Letters*, vol. 16, no. 4, pp. 564–567, 2012.

[17] O. Popoola, F. Ogunkoya, W. Popoola, R. Ramirez-Iniguez, and S. Sinanović, "Indoor localization based on multiple LEDs position estimation," in *Signal Processing Advances in Wireless Communications (SPAWC), 2016 IEEE 17th International Workshop on*. IEEE, 2016, pp. 1–6.

[18] K. Dividis, *Design and Prototyping of a Visible Light Indoor Positioning System*. Citeseer, 2007.

[19] A. Papapostolou and H. Chaouchi, "Scene analysis indoor positioning enhancements," *annals of telecommunications-annales des télécommunications*, vol. 66, no. 9-10, pp. 519–533, 2011.

[20] M. Ajmani, S. Sinanović, and T. Boutaleb, "Optimal beam radius for LED-based indoor positioning algorithm," in *Students on Applied Engineering (ISCAE), International Conference for*. IEEE, 2016, pp. 357–361.

[21] N. Abramson, "THE ALOHA SYSTEM: another alternative for computer communications," in *Proceedings of the November 17-19, 1970, fall joint computer conference*. ACM, 1970, pp. 281–285.

[22] S.-Y. Jung, S. Hann, and C.-S. Park, "TDOA-based optical wireless indoor localization using LED ceiling lamps," *IEEE Transactions on Consumer Electronics*, vol. 57, no. 4, pp. 1592–1597, 2011.

[23] W. Gu, W. Zhang, M. Kavehrad, and L. Feng, "Three-dimensional light positioning algorithm with filtering techniques for indoor environments," *Optical Engineering*, vol. 53, no. 10, pp. 107 107–107 107, 2014.

[24] M. Yasir, S.-W. Ho, and B. Vellambi, "Indoor position tracking using multiple optical receivers," *Journal of Lightwave Technology*, vol. 34, no. 4, pp. 1166–1176, 15 February 2016.

[25] Y. Xu, J. Zhao, J. Shi, and N. Chi, "Reversed three-dimensional visible light indoor positioning utilizing annular receivers with multi-photodiodes," *Sensors*, vol. 16, no. 8, p. 1254, 2016.

[26] S.-H. Yang, E.-M. Jung, and S.-K. Han, "Indoor location estimation based on LED visible light communication using multiple optical receivers," *IEEE Communications Letters*, vol. 17, no. 9, pp. 1834–1837, 2013.

[27] M. Ajmani, T. Boutaleb, and S. Sinanović, "Optical wireless communication based two receiver indoor positioning algorithm," in *Wireless Communications and Mobile Computing Conference (IWCMC), 2017 13th International*. IEEE, 2017, pp. 653–658.

[28] M. Di Renzo, H. Haas, A. Ghrayeb, S. Sugiura, and L. Hanzo, "Spatial modulation for generalized MIMO: Challenges, opportunities, and implementation," *Proceedings of the IEEE*, vol. 102, no. 1, pp. 56–103, 2014.

[29] O. R. Popoola, W. O. Popoola, R. Ramirez-Iniguez, and S. Sinanović, "Design of improved IR protocol for LED indoor positioning system," in *Wireless Communications and Mobile Computing Conference (IWCMC), 2017 13th International*. IEEE, 2017, pp. 882–887.

[30] A. E. Masson, S. Hignett, and D. E. Gyi, "Anthropometric study to understand body size and shape for plus size people at work," *Procedia Manufacturing*, vol. 3, pp. 5647–5654, 2015.

Olaoluwa R. Popoola (S'09) received the M.Eng degree in electrical and electronics engineering from the Federal University of Technology, Akure, (FUTA) Nigeria and is currently at Glasgow Caledonian University, U.K. working towards a PhD under the supervision of Dr Sinan Sinanović.

He joined the Federal University of Technology, Akure as a research assistant in 2013 and was made an assistant lecturer in 2015. His research interest is in the use of optical wireless communications for indoor positioning. He is a member of the institution of engineering technology and awards he has received include first prize cowbell mathematics competition, Ikorodu Nigeria, FUTA impact award, the Nigerian federal government scholarship award and FUTA departmental best graduating student award.

This article has been accepted for publication in a future issue of this journal, but has not been fully edited. Content may change prior to final publication. Citation information: DOI 10.1109/ACCESS.2018.2801626, IEEE Access

Sinan Sinanović received the Ph.D. degree in electrical and computer engineering from Rice University, Houston, TX, in 2006. In 2006, he joined Jacobs University Bremen, Germany, as a Post-Doctoral Fellow. In 2007, he joined The University of Edinburgh, U.K., where he was a Research Fellow with the Institute for Digital Communications. While with Halliburton Energy Services, he has developed acoustic telemetry receiver, which was patented. He was also with Texas Instruments on the development of ASIC testing. He joined Glasgow Caledonian University in 2013. His research interests cover wireless communications, interference mitigation, optical wireless, spatial modulation, and anomaly detection. He is a member of the Tau Beta Pi Engineering Honour Society and the Eta Kappa Nu Electrical Engineering Honour Society. He received the honourable mention at the International Math Olympiad in 1994.